Inorganic Chemistry Communications 102 (2019) 95–103

Contents lists available at ScienceDirect

Inorganic Chemistry Communications

journal homepage: www.elsevier.com/locate/inoche

Short communication

Monofunctional supramolecular Pt(II) complexes: Synthesis, single crystal structure, anticancer activity, *E. coli* growth retardation and DNA interaction study

Faiz-Ur Rahman[a,b], Amjad Ali[c,d], Inam Ullah Khan[e], Muhammad Zeeshan Bhatti[c,f], Manuel Petroselli[b], Hong-Quan Duong[g], Javier Martì-Rujas[h], Zhan-Ting Li[a], Hui Wang[a,*], Dan-Wei Zhang[a,*]

[a] Department of Chemistry, Fudan University, 2005 Songhu Road, Shanghai 200438, China
[b] Center for Supramolecular Chemistry and Catalysis, Department of Chemistry, Shanghai University, Shanghai 200444, China
[c] Shanghai Key Laboratory of Regulatory Biology, Institute of Biomedical Sciences, School of Life Sciences, East China Normal University, 500 Dongchuan Road, Shanghai 200241, China
[d] Institute of Integrative Biosciences, CECOS University of IT and Emerging Sciences, Peshawar, KPK, Pakistan
[e] Laboratory of Molecular Immunology, State Key Laboratory of Genetic Engineering, School of Life Sciences, Fudan University, 220 Handan Road, Shanghai 200433, China
[f] Department of Biological Sciences, National University of Medical Sciences, Rawalpindi 46000, Pakistan
[g] Institute of Research and Development, Duy Tan University, K7/25 Quang Trung, Danang 550000, Vietnam
[h] Dipartimento di Chimica, Materiali e Ingegneria Chimica – "Giulio Natta", Politecnico di Milano, Via Luigi Mancinelli 7, Milan 20131, Italy

GRAPHICAL ABSTRACT

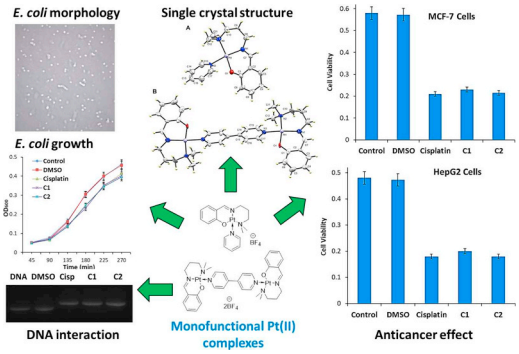

ARTICLE INFO

Keywords:
Supramolecular Pt(II) complexes
Anticancer effect of Pt(II) complexes
E. coli growth retardation
DNA interaction

ABSTRACT

Two new monofunctional mono-metallic *trans*-Pt(II)(salicylaldimine)(pyridine)·BF_4 (**C1**) and supramolecular dimetallic *trans*-(Pt(II)(salicylaldimine))$_2$(4,4-bipyridine)·$2BF_4$ (**C2**) complexes were designed and synthesized through ancillary chloride ligand exchange strategy and structurally characterized by spectroscopic, spectrophotometric and single crystal X-ray analyses. The solid-state structure analyses revealed interactions between the coordination planes, inter-molecular H-bonding, bonding in the ligand hydrogen and BF_4 anions and supramolecular interactions with solvent molecules in crystal packing. The *in vitro* anticancer effect of these complexes was investigated in breast (MCF-7) and liver (HepG2) cancer cells. Both these complexes showed significant anticancer effect comparable to cisplatin. Similarly, the effect of these complexes on *Escherichia coli*

* Corresponding authors.
E-mail addresses: wanghui@fudan.edu.cn (H. Wang), zhangdw@fudan.edu.cn (D.-W. Zhang).

https://doi.org/10.1016/j.inoche.2019.02.011
Received 28 October 2018; Received in revised form 2 February 2019; Accepted 3 February 2019
Available online 04 February 2019
1387-7003/

(*E. coli*) growth retardation was also analyzed and the results revealed stronger growth retardation effect and elongated morphology of bacterial cells in similar fashion as observed for cisplatin. The DNA interaction of **C1** and **C2** was investigated by gel electrophoresis using pET28 as target DNA. These complexes retarded migration of DNA across the gel showing their interaction with DNA.

Supramolecular multinuclear platinum(II) complexes bearing conjugated aromatic ligands are of wide interest due to their important applications in the fields of catalysis, anticancer drugs, supramolecular assemblies, sensing of different analytes and unique photo physical properties [1–4]. In these multinuclear platinum complexes, metal centers interact with each other through the coordinating ligands that interwove them together and feature their interesting properties as compared to the related mononuclear complexes [5–7]. Furthermore, multinuclear complexes of primary amine ligands and multi-pyridine donor ligands have received increasing attention because of their special biological effect in terms of DNA interaction and *in vitro* apoptotic cell death [8,9]. The activation of multiple apoptotic pathways in cancer cells and multi-targeted mechanisms inside cells increased the efforts of chemical scientists in the advancement of multi-metal supramolecular platinum-based antitumor agents [7,10,11].

Cisplatin was approved as an anticancer drug almost five decades ago and is used for almost all kinds of solid tumor [12,13]. The clinical success and extensive research on cisplatin not only revealed its effectiveness in healing of cancer patients but also revealed a number of related disadvantages [14–18]. To overcome some of these related disadvantages, there were other four platinum based anticancer drugs approved globally (carboplatin and oxaliplatin) or locally (nedaplatin and lobaplatin), all these drugs were based on identical Pt(II) center while different in terms of the attached organic assembly. The positive development in decrease in side effects of cisplatin by changing the coordinating assembly around platinum center opened a new area of platinum anticancer complexes and further searches for safer, targeted and easily synthesized effective chemotherapeutic agents were continued [15,19–22]. A number of platinum complexes were reported with better anticancer potentials and other important features, some of them are under clinical trials [23–25].

The serendipity of cisplatin was somewhat related to the growth inhibition of (*Escherichia coli*) *E. coli* cells induced by cisplatin, as Rosenberg et al. discovered it by using platinum electrode in electrochemical cell [19,26–29] Similarly many studies revealed the use of *E. coli* in preliminarily screening of biological effect of platinum complexes [30–33]. Recently, this kind of bacterial growth inhibition analyses was involved in most of the anticancer drugs development strategies [24].

Recently, we dedicated our efforts to the development of salicylaldimine based supramolecular Pt(II) complexes and their application in photo-physical and biological fields [34–38]. Herein we report related monofunctional supramolecular Pt(II) complexes, their synthesis, solid state single crystal X-ray structures, anticancer effect in multiple human cancer cells, *E. coli* growth retardation effect and DNA interaction.

Pt-1 was prepared by using our previously reported protocol [34]. The ancillary chloride ligand in **Pt-1** was removed by treating it with $AgBF_4$ in acetonitrile and further treatment with pyridine (for **C1**) or 4,4-bipyridine (for **C2**) produced these two complexes in good yields (Scheme 1) [39]. Their structures were determined by ^{1}H, ^{19}F and ^{13}C NMR spectroscopy, high resolution electrospray ionization mass spectrometry (HR ESI-MS) and elemental analyses (ESI Figs. S1–8).

X-ray quality single crystals of **C1** and **C2** were obtained from the solutions of each complex in CH_2Cl_2–*n*-hexane (1:1) mixture by slow evaporation at rt. The ORTEP plots of **C1** and **C2** were displayed in Fig. 1 while experimental details were summarized in Table 1. **C1** was crystallized in monoclinic while **C2** was in triclinic crystal systems. Each Pt metal adopted square planar environment in both of the complexes. Single crystal structures of both complexes were comprised of discrete ions of these compounds bonded together through van der Waals interactions (Figs. 3, 4, Tables S2–3). The asymmetric unit of **C1** was containing only one molecule and one BF_4 anion, while that of **C2** was consisted of two symmetry related molecules together with two BF_4 anions and two CH_2Cl_2 solvent molecules taking place in the intermolecular interactions in the crystal structure. Platinum coordination spheres were square planar consisted of O(1), N(1) and N(2) coordinated atoms of the salicylaldimine and N(3) of the pyridine (**C1**) or 4,4-bipyridine (**C2**) co-ligands (Fig. 1). Selected bond lengths and angles for **C1** and **C2** were summarized in Tables 2 and 3 respectively.

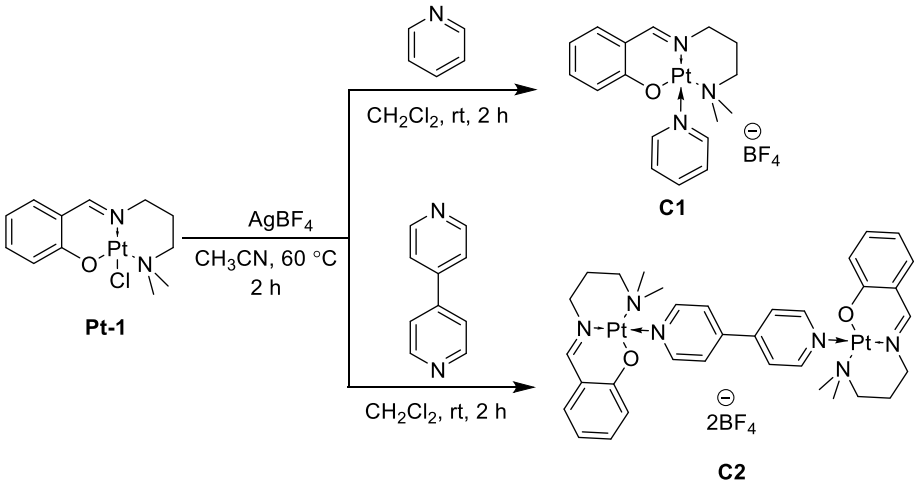

Scheme 1. Synthesis of **C1** and **C2**.

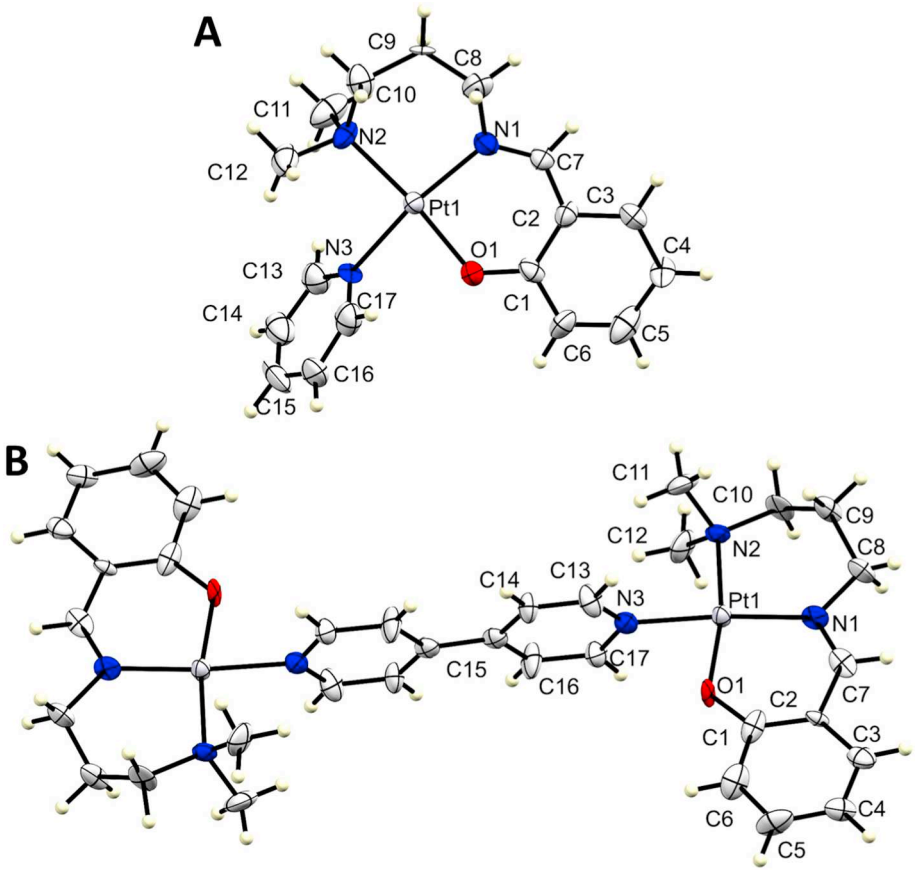

Fig. 1. ORTEP plot of single crystal at 50% probability of the thermal ellipsoids of (A) **C1** and (B) **C2**; anions and solvent molecules were omitted for clarity.

Table 1
Experimental details for **C1** and **C2**.

	C1	**C2**
CCDC no.[a]	1,874,974	1,874,975
Molecular formula	$C_{17}H_{22}BF_4N_3OPt$	$C_{36}H_{46}B_2Cl_4F_8N_6O_2Pt_2$
M [g mol^{-1}]	566.27	1300.39
T [K]	223(2)	173(2)
Crystal system	Monoclinic	Triclinic
Space group	P 2_1/c	P-1
a [Å]	9.1006(17)	9.0228(19)
b [Å]	10.4192(19)	11.975(3)
c [Å]	20.195(4)	33.036(7)
α [°]	90	81.729(3)
β [°]	92.742(3)	85.706(4)
γ [°]	90	72.924(3)
V (Å^3)	1912.7(6)	3374.5(12)
Z	4	3
Density (cal.) (mg m^{-3})	1.966	1.920
μ (Mo-$K_α$) (mm^{-1})	7.385	6.522
F(000)	1088	1878
Crystal size [mm^3]	0.500 × 0.370 × 0.110	0.160 × 0.100 × 0.080
θ range [°]	2.200 to 27.305	0.623 to 25.999
Index ranges	−10 ≤h ≤11, −13 ≤k ≤13, −23 ≤l ≤25	−11 ≤h ≤11, −12 ≤k ≤14, −40 ≤l ≤40
Reflections collected	11,701	21,801
Independent reflections	4226 [R(int) = 0.0552]	13,015 [R(int) = 0.0434]
Completeness to theta = 25.242° [%]	98.8	98.0
Absorption correction	Semi-empirical from equivalents	Semi-empirical from equivalents
Max. and min. transmission	0.746 and 0.161	0.746 and 0.436
Refinement method	Full-matrix least-squares on F^2	Full-matrix least-squares on F^2
Data/restraints/parameters	4226/30/247	13,015/132/817
Final R indices [*I* > 2sigma(I)]	R1 = 0.1033, wR2 = 0.2932	R1 = 0.0707, wR2 = 0.2160
R indices (all data)	R1 = 0.1137, wR2 = 0.3088	R1 = 0.0993, wR2 = 0.2696
Extinction coefficient	0.0013(8)	n/a
Largest diff. peak and hole	7.770 and −8.381 e·Å^{-3}	4.977 and −3.076 e·Å^{-3}

[a] Crystallographic data for **C1**, CCDC 1874974 and **C2**, CCDC 1874975, can be obtained from Cambridge Crystallographic Data Center 12 Union Road, Cambridge CB2 1EZ, UK; Tel: +44-1223336408; fax: +44-1223336003; e-mail: deposit@ccdc.cam.ac.uk.

Table 2
Selected bond lengths (Å) and angles (°) of **C1**.

Bond lengths		
1	Pt(1)–O(1)	1.981(10)
2	Pt(1)–N(1)	2.025(12)
3	Pt(1)–N(3)	2.062(11)
4	Pt(1)–N(2)	2.087(12)
Bond angles		
5	∠O(1)-Pt(1)-N(1)	91.7(5)
6	∠O(1)-Pt(1)-N(3)	80.4(4)
7	∠N(1)-Pt(1)-N(3)	172.0(5)
8	∠O(1)-Pt(1)-N(2)	173.5(5)
9	∠N(1)-Pt(1)-N(2)	94.5(5)
10	∠N(3)-Pt(1)-N(2)	93.4(5)

Pt—O bond lengths were observed to be the shortest in both of the complexes showed the covalent nature of these bonds (Table 2 entry 1 and Table 3 entry 1, 5 and 9). The longest bond length was observed for the bond between Pt(II) and the second nitrogen atom of the salicylaldimine ligand (Pt-N(2)), in which it was the effect of the longer propane chain of amine part of the salicylaldimine ligand (Table 2 entry 4 and Table 3 entry 4, 8 and 12). The bond lengths of the other donor atoms and Pt(II) atoms were almost equal in both **C1** and **C2**. The sum of the angles around each Pt(II) atom was calculated to be 360°. The angle based on Pt(II) atom and the two donor nitrogens of the salicylaldimine part of the ligand ($\angle N_1Pt_1N_2$) was observed as the biggest one showing the effect of the strain of the longer chain between the two nitrogens, that gives certain orientation to the longer propane chain (Table 2 entry 9 and Table 3 entry 17, 23 and 30). The angles based on salicylaldimine part O-donor atom, Pt(II) atom and the co-ligand (pyridine, 4,4-bipyridine) N-donor atom in both **C1** and **C2** were observed to be the smallest ones representing slight repulsion of the bulky dimethylamine group for the co-ligand that is pushed to the opposite side resulting decrease in the angular values (Table 2 entry 6 and Table 3 entry 14, 20 and 25). Other corresponding angles were compared to each other and some similarities were observed in **C1** and **C2**.

Four coordinated atoms around Pt(II) have planar orientation, similarly salicylaldimine ligand functioned as a tri-coordinated pincer, resulted in planar orientation around Pt(II) center. Co-ligand pyridine plane is almost perpendicular to salicylaldimine plane in **C1** (Fig. 2A–B). In case of **C2** each salicylaldimine ligand resulted in planar orientation, while the plane of 4,4-bipyridine is perpendicular to each Pt(II) based salicylaldimine plane (Fig. 2C).

Non-covalent interactions like hydrogen bonding π-π stacking or short interactions among different anions and cations are the most important features in supramolecular chemistry and crystal engineering. Different structures are designed for such interactions to get the desired supramolecular or crystalline materials. In **C1**, we observed strong interactions among the main complex cations and BF_4 anions (Fig. 3, Table S2). BF_4 anions were found to be associated through hydrogen bonding with different hydrogens of the salicylaldimine ligand coordinated to Pt(II) center (Fig. 3A–B) and act as bridge between the metal ligand based cations. These interactions are effective for 2D or 3D arrangements of the cations and anions in crystal packing (Fig. 3C–D).

In the crystal packing of **C2** dimerization of two conformers was observed. Different short contacts were observed among different hydrogens of the ligand, CH_2Cl_2 and BF_4 anions. CH_2Cl_2 solvent inclusion in the spaces in crystal packing lead to strong hydrogen bonding with BF_4 anions and the ligands of the next molecules give rise to the formation of a supramolecular assembly of Pt(II) based cations and BF4 anions of **C2** (Fig. 4, Table S3). Planar interactions of the salicylaldimine ligands through intermolecular hydrogen bonding between the phenolic oxygen and methylene protons of the propane chain of the imine part resulted in dimerization (Fig. 4A–D).

Breast and liver cancers are the most dangerous and prevailing types of cancer. We studied the *in vitro* anticancer effect of **C1-C2** in these two types of human cancer cells (MCF-7 and HepG2) (Fig. 5A–B). The anticancer study results revealed these complexes to have significant cytotoxicity in these cells. Cisplatin was used as a positive control in this study and we found that cytotoxicity of **C1** and **C2** was comparable to cisplatin. Compared to the less active precursor (**Pt-1**) [34], these monofunctional complexes showed better cytotoxicity in cancer cells. The effect of monometallic complex **C1** was slight lower as compared to positive control cisplatin, while the supramolecular complex **C2** showed similar cytotoxicity to cisplatin that was also higher as compared to that observed for **C1**.

We also performed dose-dependent anticancer analyses for **C1** and **C2** in HepG2 cells. Cancer cells were incubated with 5, 10 or 20 μM of cisplatin **C1** or **C2** and analyzed by MTT assay (Fig. 5C). The anticancer effect of **C1** and **C2** increased in dose dependent manner, we found good effect for 5 μM which was further increased with increasing concentration and maximum anticancer effect was observed for 20 μM of each of these Pt(II) complexes. Next time-dependent anticancer analyses for **C1** and **C2** were performed in HepG2 cells. Cancer cells were treated with 20 μM of particular complex and analyzed by MTT assay in time dependent manner (Fig. 5D). The anticancer assay's results revealed significant effect of **C1** and **C2** on cancer cell proliferation during 24 h that was further enhanced over 48 and 72 h. These results revealed stronger cytotoxic effect of **C1-C2** that resulted efficient apoptosis in

Table 3
Selected bond lengths (Å) and angles (°) of **C2**.

Bond lengths			*Bond angles*					
1	Pt(1)-O(1)	1.999(10)	13	∠O(1)-Pt(1)-N(1)	93.9(5)	25	∠O(3)-Pt(3)-N(9)	81.1(4)
2	Pt(1)-N(1)	2.008(15)	14	∠O(1)-Pt(1)-N(3)	79.2(5)	26	∠O(3)-Pt(3)-N(6)	90.1(5)
3	Pt(1)-N(3)	2.047(14)	15	∠N(1)-Pt(1)-N(3)	172.9(5)	27	∠N(9)-Pt(3)-N(6)	171.0(5)
4	Pt(1)-N(2)	2.095(12)	16	∠O(1)-Pt(1)-N(2)	169.4(5)	28	∠O(3)-Pt(3)-N(7)	174.1(5)
5	Pt(2)-O(2)	2.012(10)	17	∠N(1)-Pt(1)-N(2)	96.4(5)	29	∠N(9)-Pt(3)-N(7)	93.3(5)
6	Pt(2)-N(4)	2.018(13)	18	∠N(3)-Pt(1)-N(2)	90.5(5)	30	∠N(6)-Pt(3)-N(7)	95.4(5)
7	Pt(2)-N(8)	2.022(13)	19	∠O(2)-Pt(2)-N(4)	92.3(5)			
8	Pt(2)-N(5)	2.103(13)	20	∠O(2)-Pt(2)-N(8)	80.1(5)			
9	Pt(3)-O(3)	1.987(10)	21	∠N(4)-Pt(2)-N(8)	172.4(5)			
10	Pt(3)-N(9)	2.014(12)	22	∠O(2)-Pt(2)-N(5)	171.1(5)			
11	Pt(3)-N(6)	2.016(13)	23	∠N(4)-Pt(2)-N(5)	96.6(5)			
12	Pt(3)-N(7)	2.107(11)	24	∠N(8)-Pt(2)-N(5)	91.0(6)			

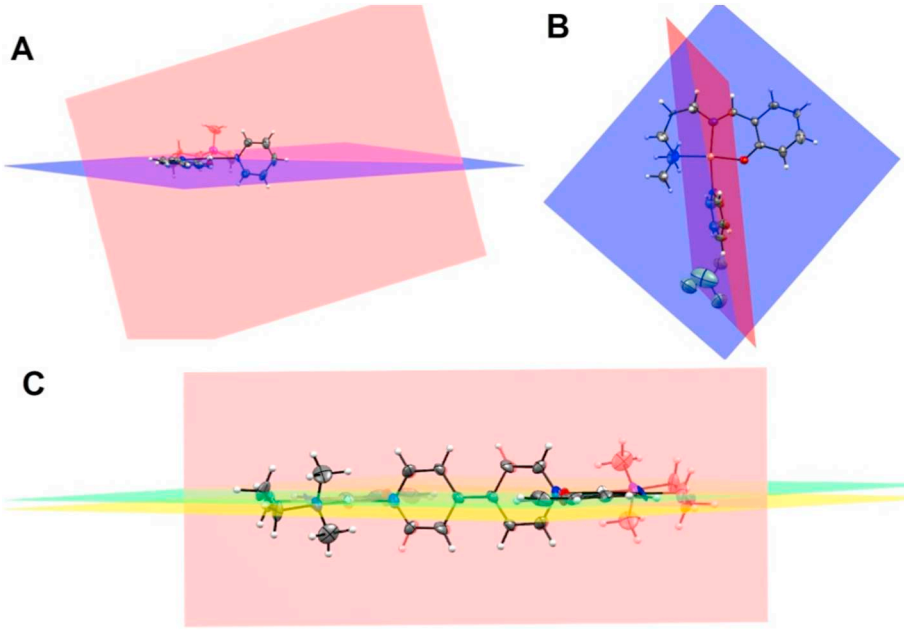

Fig. 2. Plottings of the planes of the ligand and co-ligand; In **C1** (A) and (B) planar orientations of the salicylaldimine ligand (blue) and the plane formed by co-ligand (pyridine) (pink) are shown in **C2** (C) planar orientation of two salicylaldimine ligands (green and yellow) and the orientation of co-ligand (4,4-pyridine) (pink) are shown. (For interpretation of the references to colour in this figure legend, the reader is referred to the web version of this article.)

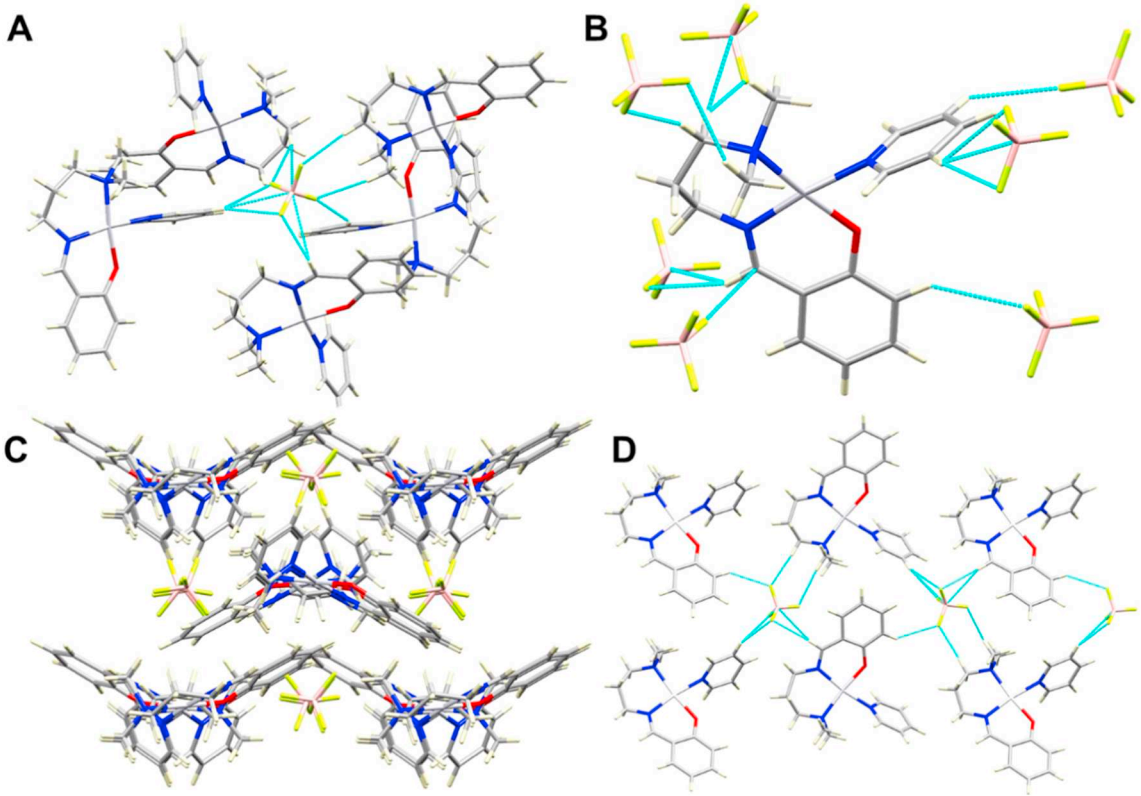

Fig. 3. Supramolecular interactions in crystal packing of **C1**; Blue bonds show short contacts and hydrogen bonds among different hydrogens and BF_4 anions, A) BF_4 anion surrounded by Pt(II) complex cation parts, B) Pt(II) complex cation parts surrounded by BF_4 anions, C) 2D arrays of cations and anions in crystal packing of **C1**, D) 1D plane formed by the arrangement of cations and anions of **C1** connected together through short contacts. (For interpretation of the references to colour in this figure legend, the reader is referred to the web version of this article.)

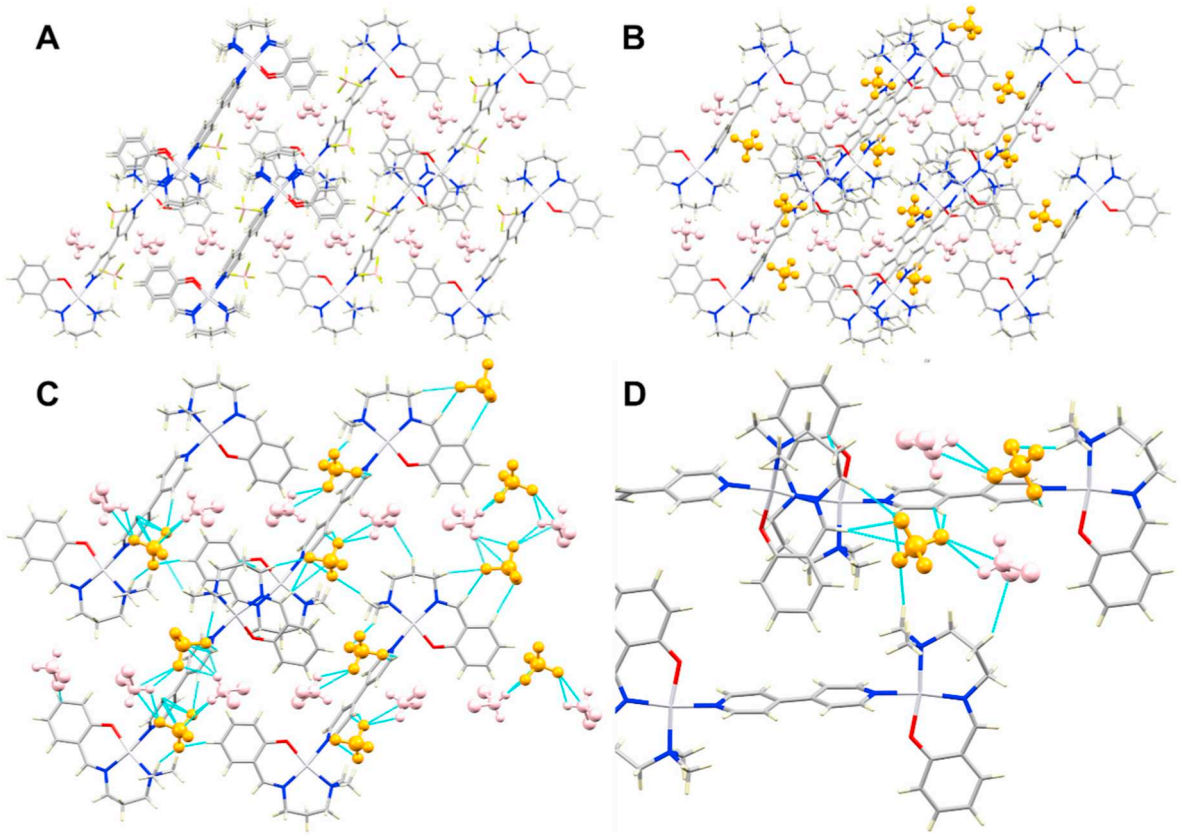

Fig. 4. Supramolecular interactions in crystal packing of **C2**; A) CH_2Cl_2 molecules (pink ball and stick style) making 1D arrays in intermolecular spaces, B) 1D arrays of BF_4 anions (orange ball and stick style) in crystal packing, C) Blue lines show short interactions among different hydrogens of the ligand, CH_2Cl_2 and BF_4 anions, D) Magnified view of the potential supramolecular short interactions among different hydrogens of the ligand, CH_2Cl_2 and BF_4 anions. (For interpretation of the references to colour in this figure legend, the reader is referred to the web version of this article.)

cancer cells while using small concentration of each complex over short time (24 h) period of incubation.

The growth retardation effect of platinum-based anticancer complexes on *E. coli* is considered a landmark experiment performed by Rosenberg et al., which is also related to the discovery of cisplatin. Platinum complexes inhibited cell division and resulted filamentous morphology in bacterial cells [24,26]. Therefore, **C1** and **C2** were assessed for their effects on growth and morphology of *E. coli*. **C1** and **C2** caused a prominent retardation in growth of bacterial cells as compared to control (Fig. 6A–D). The growth retardation effect of each complex was comparable to that of cisplatin. This was in accordance with the reported studies conducted for other platinum complexes especially cisplatin [26,28].

C1 and **C2** showed corresponding effect on morphology of *E. coli* cells (Fig. 6), control bacterial cells grew normal and healthier with clear round morphology, while bacteria treated with cisplatin, **C1** or **C2** showed elongated morphology indicated that these compounds affected morphology of the subject bacterial cells. These results also showed consistency with the other reported platinum-based anticancer compounds discussed earlier.

The primary target of platinum complexes inside cancer cells is reported to be DNA, Pt(II) interacts with DNA strands to make inter- or intra-strand complexes and stop cancer cell growth. This interaction is checked *in vitro* by gel electrophoresis. We also measured DNA interaction of **C1** and **C2** by gel electrophoresis. We found retarded migration of plasmid DNA across the gel as compared to the control DNA. The retardation effect of **C1** and **C2** was comparable to that of cisplatin (Fig. 7). These results showed a good interaction of these Pt(II) complexes with DNA to form certain metal-DNA complex, as a result its flow across the gel was decreased. Inside cancer cells, platinum complexes target DNA to form such complexes that arrest cell growth and finally kill cancer cells.

Monofunctional, mono- and di-metallic supramolecular Pt(II) complexes were prepared and characterized by single crystal X-ray analysis. Single crystal structures of these complexes revealed supramolecular interactions among different anions, cations and solvents molecules in single crystal packing. These complexes were analyzed for their *in vitro* anticancer effect in MCF-7 and HepG2 cells that showed their stronger anticancer nature. Incubation of *E. coli* with these complexes showed considerable growth retardation effect on bacteria, similarly elongated cell morphology was observed in *E. coli* cells. Slow migration of plasmid DNA across the gel revealed certain interaction of DNA and these Pt(II) complexes that showed their possible target biomolecule inside cancer cells should be DNA. To this end, **C1** and **C2** showed significant anticancer effect in cancer cells and also showed strong growth inhibitory effect in bacteria. This study can provide a preliminary base for further mechanistic *in vitro* or *in vivo* anticancer study based on these monofunctional supramolecular complexes. Moreover, mechanistic investigation on these complexes seems to be important to further explore the cytotoxic nature of these complexes against cancer cells.

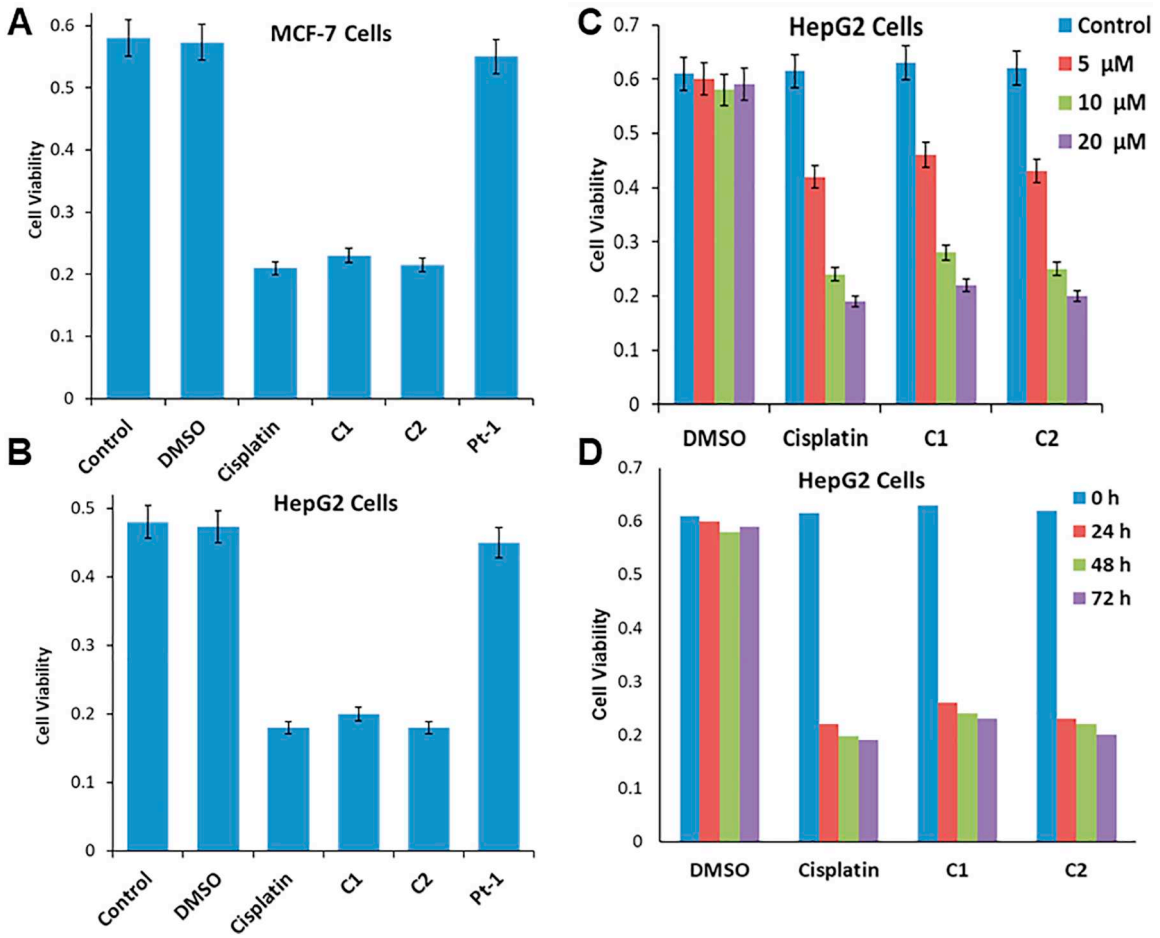

Fig. 5. MTT assay results of cytotoxic effect of **C1** and **C2**; MCF-7 (A) and HepG2 (B) cells were treated with 20 μM of cisplatin, **C1** or **C2** for 24 h and analyzed by MTT assay. (C) Dose-dependent analysis; HepG2 cells were incubated with cisplatin, **C1** or **C2** mentioned concentration for 24 h and cell viability was measured, (D) Time-dependent analysis; HepG2 cells were incubated with 20 μM of cisplatin, **C1** or **C2** and cell viability was measured at the mentioned time point. DMSO was used as a vehicle control while cisplatin was used as a positive control. Error bars represented the average of three independent experiments (mean ± s.d.)

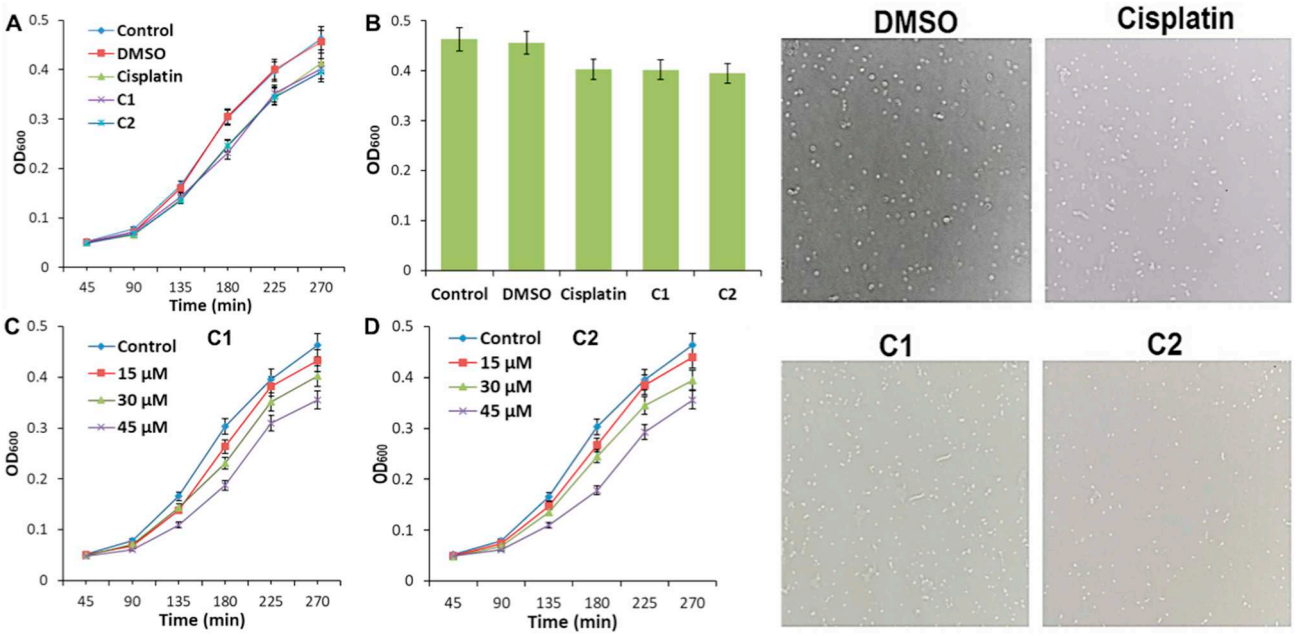

Fig. 6. Effects of **C1** and **C2** on the growth of *E. coli*; (A) Plot of cell growth (OD) *vs* time, *E. coli* was treated with 20 μM of the respective complex and OD was measured at mentioned time interval, (B) Comparison of growth inhibition at the final time point (270 min), Plot of growth (OD) *versus* time of increasing concentration (15–45 μM) of **C1** (C) and **C2** (D) on cell growth of *E. coli*, Error bars represented the average of three independent experiments (mean ± s.d.), Changes in morphology of *E. coli* observed by microscope; *E. coli* was treated with 20 μM of cisplatin, **C1** or **C2** for 4.5 h and images were taken under light microscope. Bacteria treated with Pt(II) complexes showed elongated morphology as compared to the control (DMSO treated bacteria).

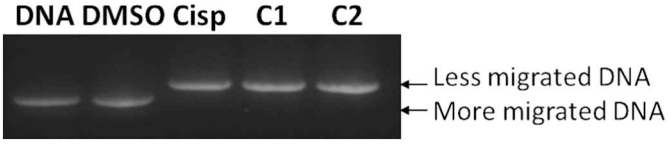

Fig. 7. C1 and **C2** interaction with plasmid DNA; pET28 plasmid DNA was incubated with **C1**, **C2** or cisplatin (20 μM) at 37 °C for 24 h and gel electrophoresed.

Acknowledgements

The authors acknowledge Ministry of Science and Technology of the People's Republic of China (2013CB834501), Science and Technology Commission of Shanghai Municipality (13NM1400200), National Natural Science Foundation of China (No. 21102017) and China postdoctoral association for providing postdoctoral fellowship.

Appendix A. Supplementary material

Supplementary data to this article can be found online at https://doi.org/10.1016/j.inoche.2019.02.011.

References

[1] M. Shiotsuka, T. Toda, K. Matsubara, Y. Itou, T. Hashimoto, Synthesis and characterization of supramolecular complexes of a tetranuclear metallocycle with platinum(II) bis-ethynylphenylethynylpyridine organometallic complexes, Transit. Met. Chem. 38 (2013) 913–922.
[2] T.C. Johnstone, K. Suntharalingam, S.J. Lippard, The next generation of platinum drugs: targeted Pt(II) agents, nanoparticle delivery and Pt(IV) prodrugs, Chem. Rev. 116 (2016) 3436–3486.
[3] J. Ni, J.-J. Kang, H.-H. Wang, X.-Q. Gai, X.-X. Zhang, T. Jia, L. Xu, Y.-Z. Pan, J.-J. Zhang, A colorimetric/luminescent benzene compound sensor based on a bis(σ-acetylide) platinum(ii) complex: enhancing selectivity and reversibility through dual-recognition sites strategy, RSC Adv. 5 (2015) 65613–65617.
[4] F. Rabilloud, M. Harb, H. Ndome, P. Archirel, UV-visible absorption spectra of small platinum carbonyl complexes and particles: a density functional theory study, J. Phys. Chem. A 114 (2010) 6451–6462.
[5] F.-U. Rahman, H. Wang, D.-W. Zhang, Z.-T. Li, 42 members new hydroquinone bridged supramolecular macrocycle and its tetra-nuclear mixed ligands Pt(II) complex: a synthetic, structural and spectroscopic investigation, Inorg. Chem. Commun. 97 (2018) 157–165.
[6] F.-U. Rahman, A. Ali, I.U. Khan, H.-Q. Duong, R. Guo, H. Wang, Z.-T. Li, D.-W. Zhang, Novel phenylenediamine bridged mixed ligands dimetallic square planner Pt(II) complex inhibits MMPs expression via p53 and caspase-dependent signaling and suppress cancer metastasis and invasion, Eur. J. Med. Chem. 125 (2017) 1064–1075.
[7] N. Wheate, J. Collins, Multi-nuclear platinum drugs: a new paradigm in chemotherapy, Curr. Med. Chem. Anticancer Agents 5 (2005) 267–279.
[8] Z. Xu, S. Swavey, Photoinduced DNA binding of a multi-metallic (Cu(II)/Ru(II)/Pt (II)) porphyrin complex, Inorg. Chem. Commun. 14 (2011) 882–883.
[9] N. Farrell, DNA binding and chemistry of dinuclear platinum complexes, Comments Inorg. Chem. 16 (1995) 373–389.
[10] S. Komeda, M. Lutz, A.L. Spek, M. Chikuma, J. Reedijk, New antitumor-active azole-bridged dinuclear platinum(II) complexes: synthesis, characterization, crystal structures and cytotoxic studies, Inorg. Chem. 39 (2000) 4230–4236.
[11] K.J. Mellish, Y. Qu, N. Scarsdale, N. Farrell, Effect of geometric isomerism in dinuclear platinum antitumour complexes on the rate of formation and structure of intrastrand adducts with oligonucleotides, Nucleic Acids Res. 25 (1997) 1265–1271.
[12] B. Lippert, Cisplatin: Chemistry and Biochemistry of a Leading Anticancer Drug, Verlag Helvetica Chimica Acta Zurich, Swithzerland, 1999.
[13] B. Rosenberg, L. Vancamp, J.E. Trosko, V.H. Mansour, Platinum compounds - a new class of potent antitumour agents, Nature 222 (1969) 385–386.
[14] B.W.J. Harper, J.R. Aldrich-Wright, The synthesis, characterisation and cytotoxicity of bisintercalating (2,2′:6′,2″-terpyridine)platinum(II) complexes, Dalton Trans. 44 (2015) 87–96.
[15] X. Wang, Z. Guo, Targeting and delivery of platinum-based anticancer drugs, Chem. Soc. Rev. 42 (2013) 202–224.
[16] M.U. Rehman, N. Ali, S. Rashid, T. Jain, S. Nafees, M. Tahir, A.Q. Khan, A. Lateef, R. Khan, O.O. Hamiza, S. Kazim, W. Qamar, S. Sultana, Alleviation of hepatic injury by chrysin in cisplatin administered rats: probable role of oxidative and inflammatory markers, Pharmacol. Rep. 66 (2014) 1050–1059.
[17] Y.I. Yang, J.H. Ahn, Y.S. Choi, J.H. Choi, Brown algae phlorotannins enhance the tumoricidal effect of cisplatin and ameliorate cisplatin nephrotoxicity, Gynecol. Oncol. 136 (2015) 355–364.
[18] O.D. Castelán-Martínez, R. Jiménez-Méndez, F. Rodríguez-Islas, M. Fierro-Evans, B.E. Vázquez-Gómez, A. Medina-Sansón, P. Clark, B. Carleton, C. Ross, C. Hildebrand, G. Castañeda-Hernández, R. Rivas-Ruiz, Hearing loss in Mexican children treated with cisplatin, Int. J. Pediatr. Otorhinolaryngol. 78 (2014) 1456–1460.
[19] B.W. Harper, A.M. Krause-Heuer, M.P. Grant, M. Manohar, K.B. Garbutcheon-Singh, J.R. Aldrich-Wright, Advances in platinum chemotherapeutics, Chem. Eur. J. 16 (2010) 7064–7077.
[20] N.J. Wheate, S. Walker, G.E. Craig, R. Oun, The status of platinum anticancer drugs in the clinic and in clinical trials, Dalton Trans. 39 (2010) 8113–8127.
[21] J. Zhao, S. Gou, F. Liu, Y. Sun, C. Gao, Anticancer potency of platinum(II) complexes containing both chloride anion and chelated carboxylate as leaving groups, Inorg. Chem. 52 (2013) 8163–8170.
[22] W.J. Guo, Y.M. Zhang, L. Zhang, B. Huang, F.F. Tao, W. Chen, Z.J. Guo, Q. Xu, Y. Sun, Novel monofunctional platinum(II) complex mono-Pt induces apoptosis-independent autophagic cell death in human ovarian carcinoma cells, distinct from cisplatin, Autophagy 9 (2013) 996–1008.
[23] T.C. Johnstone, S.J. Lippard, The chiral potential of phenanthriplatin and its influence on guanine binding, J. Am. Chem. Soc. 136 (2014) 2126–2134.
[24] T.C. Johnstone, S.M. Alexander, W. Lin, S.J. Lippard, Effects of monofunctional platinum agents on bacterial growth: a retrospective study, J. Am. Chem. Soc. 136 (2014) 116–118.
[25] G.Y. Park, J.J. Wilson, Y. Song, S.J. Lippard, Phenanthriplatin, a monofunctional DNA-binding platinum anticancer drug candidate with unusual potency and cellular activity profile, PNAS 109 (2012) 11987–11992.
[26] B. Rosenberg, E. Renshaw, L. Vancamp, J. Hartwick, J. Drobnik, Platinum induced filamentous growth in *Escherichia coli*, J. Bacteriol. 93 (1967) 716–721.
[27] E. Wong, C.M. Giandomenico, Current status of platinum-based antitumor drugs, Chem. Rev. 99 (1999) 2451–2466.
[28] B. Rosenberg, L. Vancamp, E.B. Grimley, A.J. Thomson, Inhibition of growth or cell division in *Escherichia coli* by different ionic species of platinum(IV) complexes, J. Biol. Chem. 242 (1967) 1347–1352.
[29] B. Rosenberg, L. Vancamp, T. Krigas, Inhibition of cell division in *Escherichia coli* by electrolysis products from a platinum electrode, Nature 205 (1965) 698–699.
[30] A. Nowosielska, M.G. Marinus, Cisplatin induces DNA double-strand break formation in *Escherichia coli* dam mutants, DNA Repair 4 (2005) 773–781.
[31] F. Gümüş, İ. Pamuk, T. Özden, S. Yıldız, N. Diril, E. Öksüzoğlu, S. Gür, A. Özkul, Synthesis, characterization and *in vitro* cytotoxic, mutagenic and antimicrobial activity of platinum(II) complexes with substituted benzimidazole ligands, J. Inorg. Biochem. 94 (2003) 255–262.
[32] K. Sharma, N. Fahmi, R.V. Singh, Synthesis, characterization and toxicity of new heterobimetallic complexes of platinum(II) and palladium(II), Appl. Organomet. Chem. 15 (2001) 221–226.
[33] A. Jain, B.S.J. Winkel, K.J. Brewer, *In vivo* inhibition of *E. coli* growth by a Ru(II)/Pt (II) supramolecule [(tpy)RuCl(dpp)$PtCl_2$](PF_6), J. Inorg. Biochem. 101 (2007) 1525–1528.
[34] F.-U. Rahman, A. Ali, R. Guo, Y.-C. Zhang, H. Wang, Z.-T. Li, D.-W. Zhang, Synthesis and anticancer activities of a novel class of mono- and di-metallic Pt(II)(salicylaldiminato)(DMSO or picolino)Cl complexes, Dalton Trans. 44 (2015) 2166–2175.
[35] F.U. Rahman, A. Ali, I.U. Khan, H.Q. Duong, S.B. Yu, Y.J. Lin, H. Wang, Z.T. Li, D.W. Zhang, Morpholine or methylpiperazine and salicylaldimine based heteroleptic square planner platinum (II) complexes: *in vitro* anticancer study and growth retardation effect on *E. coli*, Eur. J. Med. Chem. 131 (2017) 263–274.
[36] F.U. Rahman, M.Z. Bhatti, A. Ali, H.Q. Duong, Y. Zhang, B. Yang, S. Koppireddi, Y. Lin, H. Wang, Z.T. Li, D.W. Zhang, Homo- and heteroleptic Pt(II) complexes of ONN donor hydrazone and 4-picoline: a synthetic, structural and detailed mechanistic anticancer investigation, Eur. J. Med. Chem. 143 (2017) 1039–1052.
[37] S.K. Khalil, A. Qadeer, Y. Huang, S. Wu, F.-U. Rahman, M. Liu, A new tetra-nuclear sulphate bridged macrocyclic Cu^{2+} complex $Cu_4(SalTCB)_4(SO_4)_2$ of salicylaldehyde/dithiocarbazate derived ligand and investigation in colorimetric Cu^{2+} sensing, Inorg. Chem. Commun. 92 (2018) 136–140.
[38] F.-U. Rahman, A. Ali, I. Khan, R. Guo, L. Chen, H. Wang, Z.-T. Li, Y. Lin, D.-W. Zhang, Synthesis and characterization of *trans*-Pt(II)(salicylaldimine)(pyridine/pyridine-4-carbinol)Cl complexes: *In vivo* inhibition of *E. coli* growth and *in vitro* anticancer activities, Polyhedron 100 (2015) 264–270.
[39] 44 mg 0.1 mmol of **Pt-1** and 30 mg, 0.15 mmol of $AgBF_4$ were taken in 20 mL of CH_3CN and refluxed at 60 °C during 2 h, during this time a white solid (AgCl) was precipitated. The mixture was vacuum evaporated to dryness. The solid recovered was dissolved in 20 mL of CH_2Cl_2 and filtered through a bed of celite that was further washed with 10 mL CH_2Cl_2. The yellowish filtrate recovered was added with excess (2 drops) of pyridine (in case of **C1**) or 0.05 mmol, 8 mg of 4,4-bipyridine (in case of **C2**). This mixture was stirred at rt for 2 h, evaporated to dryness and a yellow solid was recovered. The solid was passed through a 2 x 5 cm silica column eluted with 1–5 % CH_3OH-CH_2Cl_2. After evaporation of the volatiles **C1** (light yellow solid) or **C2** (yellow solid) was recovered which was further purified by

recrystallization from CH_2Cl_2-n-hexane. **C1:** 46 mg, 81% yield. HRMS (ESI): Calcd for $C_{17}H_{22}N_3OPtBF_4$: 566.1445, Found: 479.1412 $[M - BF_4]^+$. Anal. found (calcd) for $C_{17}H_{22}N_3OPtBF_4$: C, 35.95 (36.06); H, 3.98 (3.92); N, 7.38 (7.42). ^{1}H NMR (400 MHz, DMSO-d_6) δ 9.06 (d, J = 5.0 Hz, 2H), 8.22 (s, 1H), 8.15 (t, J = 7.7 Hz, 1H), 7.73 (t, J = 6.2 Hz, 2H), 7.44 (d, J = 7.9 Hz, 1H), 7.27 (t, J = 7.7 Hz, 1H), 6.64 (t, J = 7.4 Hz, 1H), 6.51 (d, J = 8.4 Hz, 1H), 3.92 – 3.85 (m, 2H), 3.04 – 2.94 (m, 2H), 2.62 (s, 6H), 2.08 (m, 2H) ppm. ^{19}F NMR (375 MHz, DMSO-d_6) δ -148.2 ppm. ^{13}C NMR (100 MHz, DMSO-d_6) δ 162.4, 162.0, 153.5, 140.6, 135.4, 134.5, 127.3, 120.7, 119.4, 116.9, 64.7, 59.8, 54.5, 25.1 ppm. **C2:** 43 mg, 76% yield. HRMS (ESI): Calcd for $C_{34}H_{42}N_6O_2Pt_2.2BF_4$: 1130.2740, Found: 1043.2685 $[M - BF_4]^+$. Anal. found (calcd) for $C_{17}H_{21}ClN_2O_2Pt{\cdot}1/4CH_2Cl_2$: C, 36.08 (36.12); H, 3.81 (3.74); N, 7.39 (7.43). ^{1}H NMR (400 MHz, DMSO-d_6) δ 9.32 (d, J = 5.9 Hz, 4H), 8.31 (d, J = 6.1 Hz, 4H), 8.25 (s, 2H), 7.46 (d, J = 7.5 Hz, 2H), 7.30 (t, J = 7.4 Hz, 2H), 6.67 (t, J = 7.4 Hz, 2H), 6.53 (d, J = 8.4 Hz, 2H), 3.91 (s br., 4H), 3.03 (s br., 4H), 2.69 (s, 12H), 2.11 (s br., 4H) ppm. ^{19}F NMR (375 MHz, DMSO-d_6) δ -143.5. ^{13}C NMR (100 MHz, DMSO-d_6) δ 167.2, 166.9, 159.1, 150.4, 140.2, 139.3, 129.7, 125.5, 124.0, 121.8, 69.4, 64.6, 59.4, 29.9 ppm.